

Tracer diffusion in a crowded cylindrical channelRajarshi Chakrabarti,^{*} Stefan Kesselheim, Peter Košovan,[†] and Christian Holm[‡]
Institut für Computerphysik, Universität Stuttgart, Allmandring 3, 70569 Stuttgart, Germany

(Received 19 December 2012; published 19 June 2013)

Based on a coarse-grained model, we carry out molecular dynamics simulations to analyze the diffusion of a small tracer particle inside a cylindrical channel whose inner wall is covered with randomly grafted short polymeric chains. We observe an interesting transient subdiffusive behavior along the cylindrical axis at high attraction between the tracer and the chains, however, the long-time diffusion is always normal. This process is found to be enhanced for the case that we immobilize the grafted chains, i.e., the subdiffusive behavior sets in at an earlier time and spans over a longer time period before becoming diffusive. Even if the grafted chains are replaced with a frozen sea of repulsive, nonconnected particles in the background, a transient subdiffusion is observed. The intermediate subdiffusive behavior only disappears when the grafted chains are replaced with a mobile background sea of mutually repulsive particles. Overall, the long-time diffusion coefficient of the tracer along the cylinder axis decreases with an increase in system volume fraction, the strength of the attraction between the tracer and the background, and also on freezing the background.

DOI: [10.1103/PhysRevE.87.062709](https://doi.org/10.1103/PhysRevE.87.062709)

PACS number(s): 87.10.Tf, 87.15.hj

I. INTRODUCTION

Diffusion in a crowded environment has been an active area of experimental and theoretical research [1–11]. Especially in biology it is not uncommon to find aqueous crowded environments with agents that are important for biological functions. Many examples where crowding and/or a sticky interaction between the diffusing species and the surroundings changes the rate and even the nature of the diffusion process have been found in biological or synthetic contexts.

DNA-binding proteins search for specific binding sites on a DNA molecule by combining one-dimensional diffusion along the DNA strand and three-dimensional diffusion in the bulk [7,10]. The self-diffusivity of proteins in crowded solutions has been shown to be slowed down to one fifth of the dilute limiting value [11]. Also the diffusion of proteins across the nuclear pore complex (NPC) [12–18] is an example of diffusion in a crowded environment where the crowding is due to the presence of proteins called nucleoporins that are rich in hydrophobic amino acids and form a brush [19,20] or a reversible hydrogel [20,21]. Proteins diffusing through a NPC bind to these nucleoporins and experience a slowdown. A thorough explanation of this effect would lead to a better understanding of the biological functioning of the NPC [8,21]. Very recently Kowalczyk *et al.* [18] showed how one can actually make nanopores resembling a NPC and monitor the transport of proteins through such a biomimetic nanopore.

Another issue is the emergence of non-Fickian, anomalous diffusion in the presence of crowding [1]: Evidence of anomalous diffusion was found for colloidal tracer particles in entangled actin filament networks [6] and for soluble proteins in highly viscoelastic cytoplasm and nucleoplasm [22], but

also in the case of the diffusion of small molecules in glassy polymers [23]. Very recently it has been shown that diffusion inside the NPC could also be anomalous [24]. On the other hand, a sticky interaction can also lead to subdiffusive behavior even in the absence of crowding. It has been shown experimentally that functionalized colloidal particles with DNA sticky ends diffuse anomalously on a complementarily coated surface [25]. Diffusion in hydrogels and gel-like media [26–29] are also examples of diffusion in a crowded environment, and subdiffusive behavior in an intermediate time scale has been observed in computer simulations [26] and signatures of subdiffusive behavior have been observed experimentally [3].

These observations suggest that similar physical principles govern the diffusion processes under very different conditions. We investigate these principles in a simple and generic model and shed light on the role of crowding and sticky interactions by means of molecular dynamics simulations.

We study the diffusion of tracer particles inside a cylindrical channel grafted with polymeric chains from the inside. The study of tracer dynamics inside a cylindrical channel grafted with chains needs to be carried out, although the tracer dynamics in a polymer matrix has been studied extensively by means of computer simulations [23,30–34]. Examples include diffusion of small molecules such as O₂, H₂, N₂ in short polymers [30] or in dense polymers subject to thermal motion [23], penetrants in amorphous polymers [31], or ethylbenzene in polystyrene [34]. The polymeric chains consist of mutually repulsive monomers connected with springs. In the field of polymer science, this is a typical model for a polymer in a good solvent [35]. Tracers are added to the system and the impact of their interaction with the polymer chain on their diffusional property is studied. The thermal effects of the surrounding water is replaced by a standard Langevin thermostat. In this sense it is a solvent-implicit model where hydrodynamic effects are neglected.

From a biological perspective this model, although very simple, is inspired by the brush model of the central plug of a NPC [36]. Nucleoporins rich in hydrophobic units form a brushlike structure [21] and it is believed that proteins being

^{*}Present address: Department of Chemistry, Indian Institute of Technology Bombay, Powai, Mumbai 400076, India.

[†]Present address: Department of Physical and Macromolecular Chemistry, Faculty of Science, Charles University in Prague, Czech Republic.

[‡]holm@icp.uni-stuttgart.de

transported through the central plug bind to these nucleoporins [19,37]. These bindings are believed to be hydrophobic in nature, and each binding is in the range of $1-2k_B T$ [38,39].

To mimic the aspect of crowding we have chosen a repulsive interaction between all chain monomers and the tracer particles. To investigate the role of interaction we incorporate a Lennard-Jones potential between the tracer and the monomers of which we vary the interaction strength in a range from $1k_B T$ to $2.5k_B T$ corresponding to the interaction strength of hydrophobic contacts between proteins and nucleoporins in the NPC. The resulting diffusive behavior is characterized by investigating the mean-square displacement for the tracer on different time scales.

The paper is structured as follows. In Sec. II, the model, the simulation methods, and the classification of observed diffusion processes are discussed. In Sec. III the results and interpretations for the different models are given. The paper ends with the conclusions in Sec. IV.

II. MODEL AND METHOD

The model described in the following section is evaluated using molecular dynamics. We use so-called Lennard-Jones units in which the Lennard-Jones parameter σ (see below) is chosen as the unit of length, the temperature multiplied with Boltzmann's constant is the unit of energy, and mass is measured in units of the monomer mass in the chain molecules. All quantities in the following are expressed in this unit system.

A cylinder with height 24σ and radius 9σ is created from particles with a diameter σ and a mutual distance of 1σ so that a closed cylindrical surface is formed on which each particle has four next neighbors. These particles, which we call wall particles, are fixed in space, i.e., their equations of motions are not integrated, independent of the force acting on them. The cylinder axis is chosen to be the z axis. Each of the polymeric chains is made of $N = 12$ monomers, connected through a finite extensible nonlinear elastic (FENE) potential:

$$U_{\text{FENE}}(r) = -\frac{K_f r_{\text{max}}^2}{2} \log[1 - (r/r_{\text{max}})^2]. \quad (1)$$

Here K_f is the force constant and r_{max} is the maximum displacement of the bond. In the simulation the parameters are chosen to be $K_f = 7$, $r_{\text{max}} = 2$, $N = 12$. The cylindrical surface is grafted randomly with polymeric chains by fixing the end monomer of each of the chains to one of the wall particles.

The repulsive interaction between the monomers themselves and with the wall is modeled via the purely repulsive variant of the Lennard-Jones potential, also known as the Weeks-Chandler-Andersen (WCA) potential [40]:

$$V_{\text{WCA}}(r) = \begin{cases} 4\epsilon \left[\left(\frac{\sigma}{r} \right)^{12} - \left(\frac{\sigma}{r} \right)^6 \right] + \epsilon, & \text{if } r < (2)^{1/6}\sigma, \\ 0, & \text{otherwise,} \end{cases} \quad (2)$$

with $\epsilon = 1$ and $\sigma = 1$.

The tracer particles are of the same size σ and of the same mass as the monomers. They interact with the wall particles by means of the WCA potential, and with the grafted polymers either via the WCA potential (for simple crowding), or by an

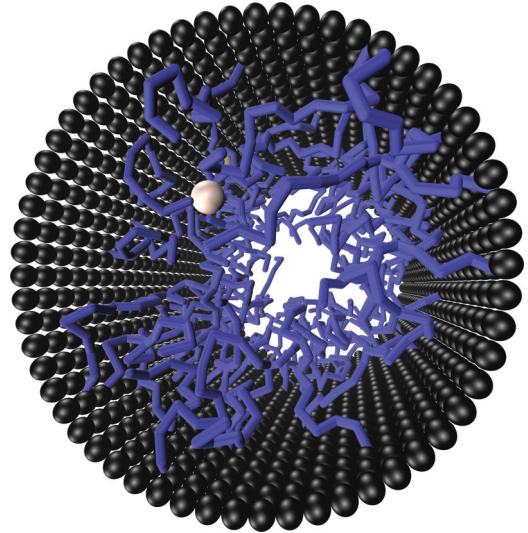


FIG. 1. (Color online) Illustration of the simulation setup. Tracer particles (white spheres) inside a cylindrical pore with rigid walls (black) grafted from inside with polymeric chains (blue/light gray). For graphical clarity the polymer chains are represented as (thinner) continuous curves, and the size of the tracer particles is exaggerated.

attractive (=“standard”) Lennard-Jones potential:

$$V_{\text{LJ}}(r) = \begin{cases} 4\epsilon \left[\left(\frac{\sigma}{r} \right)^{12} - \left(\frac{\sigma}{r} \right)^6 \right], & \text{if } r < r_{\text{cut}}, \\ 0, & \text{otherwise,} \end{cases} \quad (3)$$

where the cutoff radius is fixed at $r_{\text{cut}} = 2.5$ and the attraction strength ϵ is varied.

The degree of crowding is characterized by the grafting density γ , i.e., the number of chains per unit area of the cylinder. A typical value of $n = 75$ chains corresponds to $\gamma = 0.055$. A typical representation of the investigated system is shown in Fig. 1 by using the Visual Molecular Dynamics program (VMD) [41].

We have performed five independent simulations for each data point with $2 \times 10^6 \tau$ each in order to allow to estimate the statistical errors indicated in all figures. The time step τ is chosen to be 0.005 and a velocity Verlet algorithm is used for integration. Since the grafted chains are short, equilibration is achieved well within 5000τ . This also ensured equilibration of the tracer which was placed to the axis of the cylinder at the very beginning of the simulation. All simulations were carried out by employing a Langevin thermostat in an NVT ensemble, thus solving the full phase space stochastic equation of motion known as the Langevin equation of motion. The Langevin thermostat violates Galilean invariance and momentum conservation, and is local, hence it screens hydrodynamical interactions. As such it disturbs the true dynamics of the system, however, diffusional behavior can still be extracted if the thermostat forces are much smaller than the interparticle interactions, as in the present case. For a critical comparison of the use of the Langevin thermostat for nonequilibrium simulations of polymeric systems, see Ref. [42]. Periodic boundary conditions along the cylindrical axis are used throughout the simulation.

For a particle with mass m and the position coordinate r_i (where i stands for the i th particle), interacting with all other

particles ($i \neq j$) through a general potential $U(r_{ij})$ the full phase space Langevin equation of motion reads as

$$m \frac{d^2 \mathbf{r}_i(t)}{dt^2} = -\nabla_{\mathbf{r}_i} \sum_{j \neq i} U(\mathbf{r}_{ij}) + \mathbf{F}_i^D + \mathbf{F}_i^R, \quad (4)$$

where

$$\mathbf{F}_i^D = -m\Gamma \frac{d\mathbf{r}_i(t)}{dt} \quad (5)$$

is the frictional drag acting on the particle with friction coefficient Γ , and \mathbf{F}_i^R is the random force acting on the particle. The first moment of the random force is chosen to be zero:

$$\langle \mathbf{F}_i^R(t) \rangle = 0. \quad (6)$$

The magnitude of the random forces obeys

$$\langle \mathbf{F}_i^R(t_1) \mathbf{F}_j^R(t_2) \rangle = 6\Gamma k_B T m \delta_{ij} \delta(t_1 - t_2), \quad (7)$$

where k_B is the Boltzmann constant and T is the temperature of the Langevin thermostat.

The delta function in time between the random forces in the above equation ensures the spectrum of the random force to be white, corresponding to a Markovian process in phase space with no memory. With the above choice of random forces, a fluctuation-dissipation theorem that connects the diffusion coefficient D and the friction coefficient Γ holds: The diffusion coefficient of a single particle, up to a factor $k_B T/m$, is the inverse of the friction coefficient, $D_{\text{free}} = k_B T/(m\Gamma) = 1$. In all simulations we apply a friction coefficient of 1 and the diffusion coefficients reported in the paper are given in units of D_{free} , being also 1 in our unit system. The molecular dynamics simulations have been carried out with the help of the simulation package ESPResSo [43] in version 3.1 [44].

To describe the diffusion of tracer particles it is a common practice to use the mean-square displacement (MSD) $\langle \Delta \vec{r}_{t_0}(t)^2 \rangle$ as a measure, where $\Delta \vec{r}(t) = [\vec{r}(t+t_0) - \vec{r}(t_0)]$ is the displacement of the particle at time $t+t_0$ from its initial position at t_0 . The angular bracket denotes an average over all possible realizations of the process. Under the time translational invariance this quantity is independent of t_0 and this index can be dropped, thus t can also be interpreted as the lag time. For ergodic systems, the average over realizations can be replaced by an ensemble average. In the case of normal diffusion, MSD increases linearly with time and in d dimension reads as $\langle \Delta \vec{r}(t)^2 \rangle = 2dDt$, where D is the diffusion coefficient of the tracer particle. On the other hand, a process where the MSD is not linear in time but proportional to t^α with $\alpha \neq 1$ is referred to as anomalous or non-Fickian diffusion [1]. Here α is the diffusion exponent and if $\alpha < 1$, the process is called subdiffusive, and if $\alpha > 1$, the process is called superdiffusive. For anomalous diffusion there is no well-defined diffusion coefficient. While the definition given above is very helpful for isotropic environments, in anisotropic environments the diffusion constant needs to be replaced by a diffusion tensor. As we are only interested in the diffusive behavior along the cylinder axis (z axis), we measure the MSD in the z direction,

$$\text{MSD} = \langle [r_z(t+t_0) - r_z(t_0)]^2 \rangle, \quad (8)$$

corresponding to the zz component of the diffusion tensor. Throughout the paper D always represents the tracer diffusion

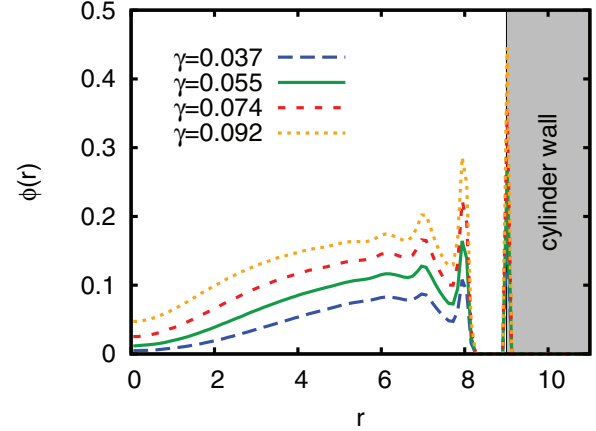


FIG. 2. (Color online) The local monomer volume fraction $\phi(r)$ at different chain grafting densities (γ) of the mobile grafted chains. Increasing the number of chains affects the density only but not the structure of the brush.

coefficient along the cylinder axis and MSD is the mean-square displacement of the tracer along the cylinder axis.

III. RESULTS

In this section, we present the results of the MD simulations. We compute the MSD of the tracer and analyze the resulting transient diffusive behavior with respect to the question if anomalous diffusion appears and try to elucidate the reasons for this by comparison to reference systems.

To explore the role of chain connectivity we compare all our results to a system when the chain monomers are not connected via the FENE potential, but free to move, thus forming a gas or a “sea” of independent particles. The other reference is a system in which the grafted chains are moving much slower than the tracer particle, and we call this a frozen background. For brevity we characterize the four possible combinations by the pairs of keywords (chains-particles) and (mobile-frozen). We will show that both properties, the chain connectivity and the background motion, have a distinct impact on the diffusion properties of the tracer particles.

First we discuss the structure of the polymer coating: The radius of gyration of the chains is ≈ 6 under all reported conditions and the mutual distance between grafting points is smaller also for the smallest grafting densities. Thus we are in the regime where the grafted chains overlap considerably. In Fig. 2 we report the local volume fractions of chain monomers, i.e., the fraction of the volume locally occupied by monomers, assuming they are spheres of diameter σ . The local volume fractions of up to 10% and more also indicate that locally the crowding is significant: Under these conditions mean free paths $\sim \sigma$ are to be expected.

A. Repulsive tracer-chain interaction

We now discuss the situation where the interaction between tracer particles and grafted chains is purely repulsive. We perform simulations with different numbers of grafted chains (n), hence different grafting densities (γ), and calculate the mean-square displacement (MSD). As we focus on the

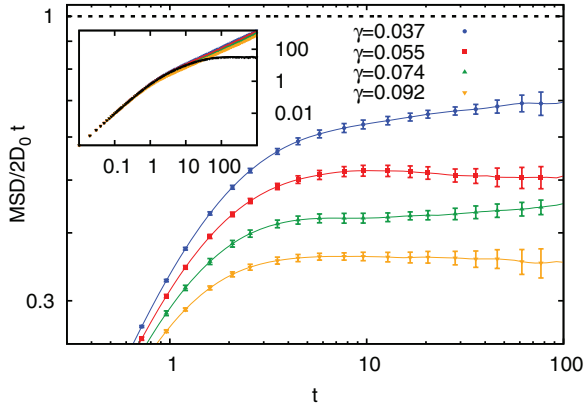


FIG. 3. (Color online) Comparison of the reduced mean-square displacement $\text{MSD}/2D_0t$ of the purely repulsive tracer along the cylinder axis of the cylinder with mobile grafted chains in the background at different chain grafting densities (γ). The diffusion constant (seen as the $t \rightarrow \infty$ limit of the curves) depends strongly on the density of grafted chains. For comparison the (nonreduced) MSD is shown in the inset. The lines corresponding to the different grafting densities are almost indistinguishable. The radial component of the MSD (shown in black) saturates.

diffusion process along the channel axes, we consider only the axial component of the MSD. In the radial direction the MSD follows closely the MSD in the axial direction for short time scales. In the long-time limit it saturates to a constant value corresponding to the square diameter of the pore. It is shown for comparison in the inset of Fig. 3. We investigate the four grafting densities seen in Fig. 3. In the double-logarithmic plot of the MSD, all lines nearly collapse (seen in the inset of Fig. 3). We thus plot the MSD of the tracer along the cylinder axis divided by $2D_0t$, where $D_0 (=D_{\text{free}})$ is the free-diffusion coefficient along the cylinder axis. Plotting this *reduced MSD* allows to see the different characteristics of diffusion. On the time scale $1/\Gamma$ a ballistic regime where the MSD is proportional to the square of t is observed, corresponding to a linear increase of the reduced MSD, and on longer time scales the diffusion becomes normal. As depicted in Fig. 3, the mean-square displacement of the tracer particles shows no sign of anomalous diffusion for all investigated grafting densities.

The long-time diffusion coefficient is reduced compared to a freely diffusing particle by collisions with the polymer chains. For low volume fractions of polymer chains we thus expect the diffusion coefficient to be reduced by a factor proportional to the (average) volume fraction, thus the probability to collide with a monomer per unit time. Neither the chain connectivity nor the question if the background moves on the same velocity scale as the tracer particles significantly influences this effect. In Fig. 4 we report the dependence of the diffusion coefficient on the monomer volume fraction, $\phi = [4/3\pi(\sigma/2)^3 Nn/\pi r_c^2 L_c]$. In all cases the tracer diffusion coefficient decreases similarly with increasing monomer volume fraction. If the monomers are connected and form chains, the impact on the diffusion coefficient is lower, as the volume from which the tracer is excluded is smaller. Also notice that the diffusion becomes faster with a mobile background than with a frozen background. This is because

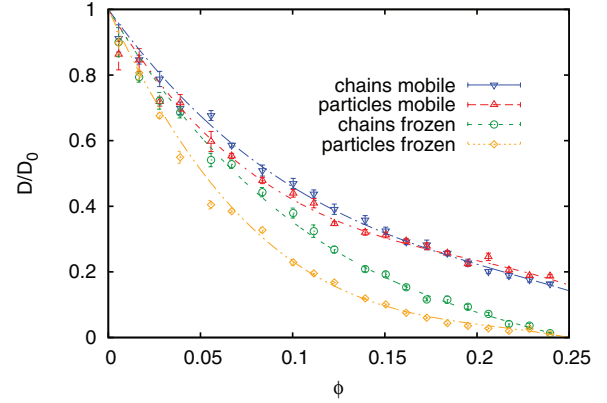


FIG. 4. (Color online) The relative diffusion coefficient D/D_0 for the purely repulsive tracers against the volume fraction of the system. The lines are guides to eyes. We compare the case where the monomers are connected by springs to form a *chain* to the case where they are isolated *particles* and the case where they are *mobile* vs the case where they are *frozen*.

in the frozen background the tracer practically collides with an infinite mass and is more likely to get bounced back to its initial position. At higher volume fractions the topology of the background becomes less important. As can be seen from Fig. 4, the two data sets corresponding to frozen particles and chains coincide at higher volume fractions as do the data sets for mobile particles and chains.

B. Attractive tracer-chain interaction

The dynamics of a tracer particle which interacts with the chains through an attractive Lennard-Jones potential as defined in Eq. (3) is more complex and shows interesting features that are missing in the case of a purely repulsive interaction. Very different modes of motion are important in the case of an attractive polymer-tracer interaction: An attractive tracer can get attached to one of the chains, follow the chain movement, move along the chain, hop from one chain to another, or hop back to the same chain. It can also move back to the bulk where it executes normal diffusion. The emerging process is a combination of all these modes of transport and should strongly depend on the strength of attraction between the tracer and the chain and also on the density of the grafted chains. We do not expect anomalous diffusion on long time scales, but see this rather as a transient phenomenon. This is what one would expect as long as the noise is white and the background is translationally invariant.

In the simulations the strength of attraction between the tracer and the polymer (ϵ) is varied from 1 to 2.5. The choice of this range of attraction is inspired by the fact that, during the transport through the NPC, proteins bind to the nucleoporins through hydrophobic contacts which are in the range of $1-2k_B T$ [39].

First we investigate the influence of the attractive interaction on the position where the tracer can be found. In Fig. 5 the probability density to find the tracer at a given distance r from the cylinder axis for different attraction strengths at a fixed grafting density 0.055 is reported. Notice that the probability of finding the tracer along the radial direction [$p(r)$] changes

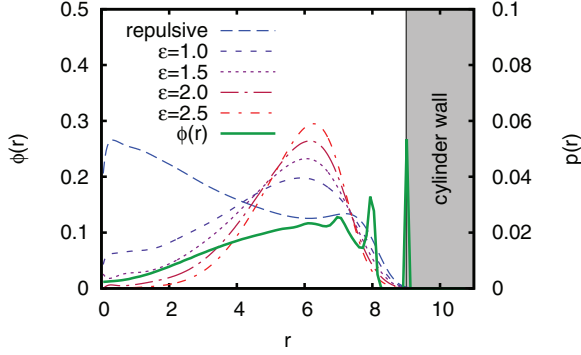


FIG. 5. (Color online) The probability of finding the tracer along the radial direction [$p(r)$] for different attraction strengths ϵ at fixed grafting density $\gamma = 0.055$. For comparison we repeat the density of monomers $\phi(r)$ from Fig. 2 (solid line). For repulsive chain-tracer interactions the tracer is pushed towards the polymer-free center of the cylinder, while the attractive interaction pulls it into the polymer brush.

profoundly on making the tracer-chain interaction attractive. In the case of purely repulsive tracers, $p(r)$ is high at the center of the cylinder ($r = 0$) and gradually decreases towards the chains and vanishes at the cylinder wall ($r = 9$). On the other hand, in the case of attractive tracers, the density profile is qualitatively different. The tracer has a low density around the center of the cylinder ($r = 0$) and has a high density close to the chains. As expected, the attractive interaction significantly pushes the tracers from the center of the cylinder towards the area of the grafted chains. For comparison we also insert the density profile $\phi(r)$ of chain monomers.

Increasing the attraction strength between the tracer particle and the chains in general slows down the diffusion. In Table I we report the long-time diffusion coefficients obtained for different attraction strengths (ϵ) at the grafting density $\gamma = 0.055$. When the attraction strength is increased, a subdiffusive regime for an intermediate time period is observed in the plot of the reduced MSD against t (Fig. 6) for $\epsilon \geq 2k_B T$.

We give the following interpretation: The energy landscape seen by a tracer particle for a fixed configuration of the polymer chain has minima in which the particle gets trapped on these intermediate time scales. These minima are especially deep in the vicinity of kinks in the polymer chain, where the attractive regions of several monomers overlap. This also occurs in the vicinity of points, where two chains closely pass by each other. When a particle gets trapped, it moves together with the monomers responsible for the trapping. Since the chains are connected, the corresponding displacement will only be

TABLE I. $\frac{D}{D_0}$ of the tracer with grafted mobile chains in the background at the grafting density $\gamma = 0.055$ for different attraction strengths (ϵ). Increased attraction strength slows down diffusion.

ϵ	$\frac{D}{D_0}$
1.0	0.38 ± 0.02
1.5	0.23 ± 0.01
2.0	0.125 ± 0.005
2.5	0.074 ± 0.003

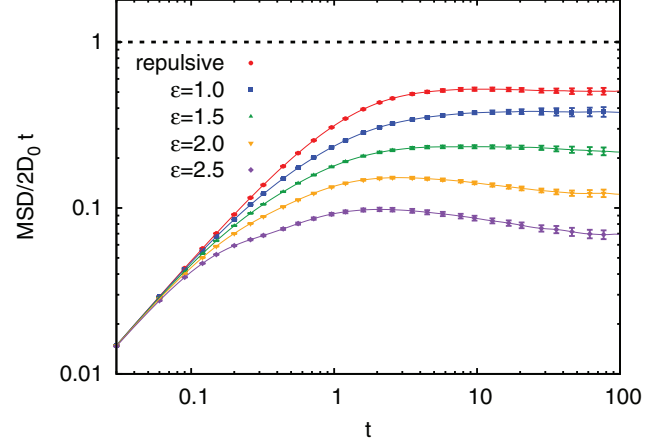


FIG. 6. (Color online) Comparison of $\text{MSD}/2D_0 t$ along the cylinder axis for the purely repulsive case and different attraction strengths (ϵ) with mobile grafted chains in the background.

small. The structure of the polymer chains itself is subject to Brownian motion, and this motion eventually helps the tracer to escape the traps.

To justify this interpretation we perform independent control experiments with a system where the chain monomers are not connected (a sea of *particles*) and investigate the impact of strongly slowing down the motion of the background, hence looking at the motion of the tracer particle on a *frozen* background. We report here only the results for attraction strength $\epsilon = 2$, but qualitatively the results that were obtained for the other investigated attraction strengths of $1k_B T$, $1.5k_B T$, and $2.5k_B T$ are similar.

The observed reduced MSDs in all four cases are shown in Fig. 7. By giving up the chain structure of the environment we expect to facilitate diffusion as the deep traps where the attractive regions of several monomers overlap are less likely as entropy drives them away from each other. The long-time diffusion coefficient is increased by a factor of 2.2 and the

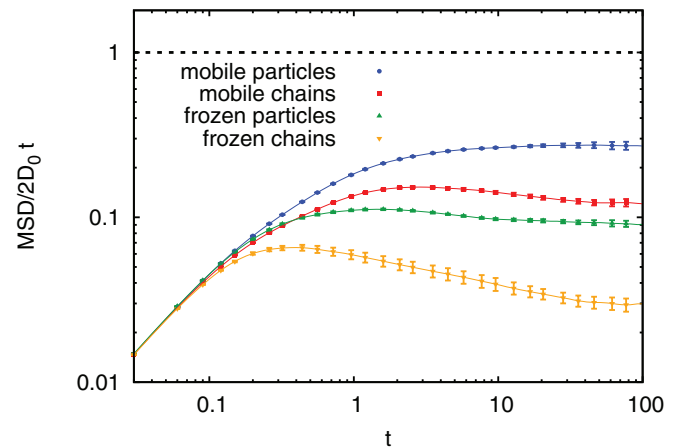


FIG. 7. (Color online) Comparison of $\text{MSD}/2D_0 t$ along the cylinder axis for different cases for $\epsilon = 2$ at the grafting density $\gamma = 0.055$. Subdiffusive transient behavior indicated by a negative slope is seen in all cases, except for the case where the monomers are not connected and allowed to move. Chain structure and freezing the background facilitates subdiffusion.

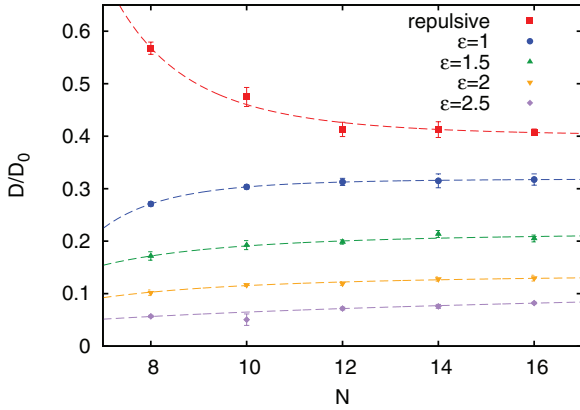


FIG. 8. (Color online) Plot of D/D_0 for the tracer at a fixed volume fraction $\sim 10\%$ against the grafted chain length (N). Lines are guides to eyes.

reduced MSD no longer exhibits any subdiffusive behavior. Fixing the position of the disconnected monomers slows down diffusion again, as this suppresses the joint diffusion of complexes of tracers and monomers, but merely stops the tracers until they can escape from their traps. For $\epsilon = 2$ this stopping effect is so pronounced that a transient subdiffusive behavior occurs (corresponding to the negative slope of the yellow curve with triangles in Fig. 7), but for weaker attraction it disappears.

Freezing the structure of the chains does not change the distribution of traps, but it changes their lifetimes. Trapped particles have to escape by their own Brownian motion and the random motion of the chains no longer facilitates their escape due to random displacements of the traps. It is seen that a substantially more pronounced subdiffusive regime occurs. The long-time diffusion coefficient is decreased by 70% by freezing the background. This observation qualitatively supports the proposition of Bickel and Bruinsma [45]. They showed with a very simple model for the transport across the NPC that the fluctuating network of chains in the background acts as an extra noise and actually enhances the diffusion of a protein immersed in it as compared to a frozen network.

C. Varying chain lengths

All the results presented above deal with a fixed chain length of the polymers ($N = 12$). But what would be the effect of varying the chain lengths while keeping the volume fraction (ϕ) fixed? We performed identical simulations as mentioned above, but with different chain lengths N and choosing the number of chains n so that a volume fraction of $\sim 10\%$ was obtained. In Fig. 8 we report the long-time diffusion coefficient as a function of the chain length. For the purely repulsive tracer the value of D/D_0 decreases by around 30% when changing the chain length from 8 to 16. Interestingly, for the attractive tracers this trend is reversed: The diffusion coefficient increases. At the highest attraction strength ($\epsilon = 2.5$) we observe an increase by almost 50%. Our explanation is as follows: For repulsive chain-tracer interactions the tracer is pushed into the center of the channel. There it can diffuse relatively freely as the local monomer

TABLE II. No subdiffusion is observed in case of purely repulsive tracers. Results for attractive tracers are summarized below.

Background	Mobile	Frozen
Chains	Transient subdiffusion at intermediate attraction	Transient subdiffusion at intermediate attraction
Particles	No subdiffusion	Transient subdiffusion at high attraction

density is reduced. Attractive interactions pull the tracer into the brush where it is slowed down. All these trends are visible (Fig. 5). Increasing the chain length changes the distribution of monomers: The short chains are too short to reach the pore axis and an empty hole appears, while for the longest chains the monomer distribution extends to the cylinder axis. For the two different cases extending the chain length has opposite consequences: For the repulsive tracer, preferably located in the low-density region in the center, additional obstacles appear that slow it down. In the case of attractive tracers, mostly sitting in the grafted brush, the brush density decreases and thus diffusion is eased. Increasing the chain length to values higher than 12 does not significantly affect the diffusion constant for the repulsive case. This indicates that our choice of $N = 12$ in the simulations shown above was sufficiently large. Our results, however, indicate that understanding the length of the nucleoporins in the NPCs can be very important for understanding the mechanisms of transport in the NPC.

IV. CONCLUSIONS

In this work, we have investigated the process of the diffusion of tracer particles inside a crowded cylindrical channel. Our coarse-grained simulations show that if the interaction between the environment and the tracer particle is purely repulsive, the diffusion is slowed down significantly: up to 80% if the background moves, and up to 95% if the background is frozen. No subdiffusive behavior is observed on any time scale. If the tracer interaction, however, is only weakly attractive ($1-2.5k_B T$), we observe a stronger slowdown than in the repulsive case, and also a pronounced subdiffusive regime. The subdiffusive regime is enlarged by freezing the background, corresponding to a much slower motion of the background particles. These findings are summarized in Table II.

Our findings suggest that the subdiffusive behavior observed by Lowe *et al.* [24] for the diffusion of tracers in the NPC is not caused by crowding from a polymer brush alone. Our results clearly demonstrate that simple attractive interactions between the crowding polymer brush and the transported particles are sufficient to observe transient subdiffusive behavior. The presence of attractive interactions was recently revealed in the work of Lim *et al.* [46] who showed that proteins that help transporting cargo through the NPC do have an attractive interaction with the nucleoporin polymers in the NPC. It, however, remained unanswered if the nucleoporins form a gel rather than a brush phase and what consequences this has for the cargo transport through the NPC. In the future we want to refine and extend our present model in this direction.

ACKNOWLEDGMENTS

Illuminating discussion with Dr. Olaf Lenz and Dr. Felix Höfling are gratefully acknowledged. We also

thank Volkswagenstiftung and the Collaborative Research Centres 716 (SFB 716) for providing the necessary financial funds.

-
- [1] I. M. Sokolov, *Soft Matter* **8**, 9043 (2012).
- [2] N. Fakhri, F. C. MacKintosh, B. Lounis, L. Cognet, and M. Pasquali, *Science* **330**, 1804 (2010).
- [3] R. Raccis, R. Roskamp, I. Hopp, B. Menges, K. Koynov, U. Jonas, W. Knoll, H.-J. Butt, and G. Fytas, *Soft Matter* **7**, 7042 (2011).
- [4] E. Fillippidi, V. Michalidou, B. Loppinet, J. Rühle, and G. Fytas, *Langmuir* **23**, 5139 (2007).
- [5] F. Höfling, K.-U. Bamberg, and T. Franosch, *Soft Matter* **7**, 1358 (2011).
- [6] I. Y. Wong, M. L. Gardel, D. R. Reichman, E. R. Weeks, M. T. Valentine, A. R. Bausch, and D. A. Weitz, *Phys. Rev. Lett.* **92**, 178101 (2004).
- [7] J.-H. Jeon, V. Tejedor, S. Burov, E. Barkai, C. Selhuber-Unkel, K. Berg-Sørensen, L. Oddershede, and R. Metzler, *Phys. Rev. Lett.* **106**, 048103 (2011).
- [8] S. Frey, R. P. Richter, and D. Görlich, *Science* **314**, 815 (2006).
- [9] J. Gorman, A. Chowdhury, J. A. Surtees, J. Shimada, D. R. Reichman, E. Alani, and E. C. Greene, *Mol. Cell* **28**, 359 (2007).
- [10] B. van den Broek, M. A. Lomholt, S. M. J. Kalisch, R. Metzler, and G. J. L. Wuite, *Proc. Nat. Acad. Sci. USA* **105**, 15738 (2008).
- [11] F. Roosen-Runge, M. Hennig, F. Zhang, R. M. J. Jacobs, M. Sztucki, H. Schober, T. Seydel, and F. Schreiber, *Proc. Natl. Acad. Sci. USA* **108**, 11815 (2011).
- [12] R. Bayliss, K. Ribbeck, A. Debra, H. M. Kent, C. M. Feldherr, D. Görlich, and M. Stewart, *J. Mol. Biol.* **293**, 579 (1999).
- [13] B. Alberts, A. Johnson, J. Lewis, M. Raff, K. Roberts, and P. Walter, *Molecular Biology of the Cell* (Garland, New York, 2002).
- [14] J. A. Cohen, A. Chaudhuri, and R. Golestanian, *Phys. Rev. Lett.* **107**, 238102 (2011).
- [15] T. A. Isgro and K. Schulten, *J. Mol. Biol.* **366**, 330 (2007).
- [16] S. P. Bird and L. A. Baker, *Biomacromolecules* **12**, 3119 (2011).
- [17] A. Zilman, S. D. Talia, B. T. Chait, M. P. Rout, and M. O. Magnasco, *PLoS Comput. Biol.* **3**, 1281 (2007).
- [18] S. W. Kowalczyk, L. Kapinos, T. R. Blosser, T. Magalhaes, P. van Nies, R. Y. H. Lim, and C. Dekker, *Nat. Nanotechnol.* **6**, 433 (2011).
- [19] S. Frey and D. Görlich, *Cell* **130**, 512 (2007).
- [20] M. Elbaum, *Science* **314**, 766 (2006).
- [21] R. Lim, N. P. Huang, J. Koser, J. Deng, K. H. Aaron-Lau, K. Schwarz-Herion, and B. Fahrenkrog, and U. Aebi, *Proc. Natl. Acad. Sci.* **103**, 9512 (2006).
- [22] G. Guigas, C. Kalla, and M. Weiss, *FEBS Lett.* **581**, 5094 (2007).
- [23] A. A. Gusev and U. W. Suter, *J. Chem. Phys.* **99**, 2228 (1993).
- [24] A. R. Lowe, J. J. Siegel, P. Kalab, M. Siu, and J. T. Liphardt, *Nature (London)* **600**, 467 (2010).
- [25] Q. Xu, L. Feng, R. Sha, N. C. Seeman, and P. M. Chaikin, *Phys. Rev. Lett.* **106**, 228102 (2011).
- [26] F. Tabatabaei, O. Lenz, and C. Holm, *Colloid Polym. Sci.* **289**, 523 (2011).
- [27] B. Amsden, *Macromolecules* **31**, 8382 (1998).
- [28] T. Cherdhirankorn, A. Best, K. Koynov, K. Peneva, K. Müllen, and G. Fytas, *J. Phys. Chem. B* **113**, 3355 (2009).
- [29] D. C. Viehman and K. S. Schweizer, *J. Phys. Chem. B* **112**, 16110 (2008).
- [30] H. Takeuchi and K. Okazaki, *J. Chem. Phys.* **92**, 5643 (1990).
- [31] F. Müller-Plathe, *J. Chem. Phys.* **94**, 3192 (1991).
- [32] C. S. Chassapis, J. K. Petrou, J. N. Petropoulos, and D. N. Theodorou, *Macromolecules* **29**, 3615 (1996).
- [33] V. A. Harmandaris, D. Angelopoulou, V. G. Mavrantzas, and D. N. Theodorou, *J. Chem. Phys.* **116**, 7656 (2002).
- [34] V. A. Harmandaris, N. P. Adhikari, N. F. A. van der Vegt, K. Kremer, B. Mann, R. Voelkel, H. Weiss, and C. Liew, *Macromolecules* **40**, 7026 (2007).
- [35] G. S. Grest and K. Kremer, *Phys. Rev. A* **33**, 3628 (1986).
- [36] S. S. Patel, B. J. Belmont, J. M. Sante, and M. F. Rexach, *Cell* **129**, 83 (2007).
- [37] M. Herrman, N. Neuberth, J. Wissler, J. Pérez, D. Gradl, and A. Naber, *Nano Lett.* **9**, 3330 (2009).
- [38] R. Moussavi-Baygi, Y. Jamali, R. Karimi, and M. R. K. Mofrad, *Biophys J.* **100**, 1410 (2011).
- [39] R. Moussavi-Baygi, Y. Jamali, R. Karimi, and M. R. K. Mofrad, *PLoS Comput. Biol.* **7**, e1002049 (2011).
- [40] J. D. Weeks, D. Chandler, and H. C. Andersen, *J. Chem. Phys.* **54**, 5237 (1971).
- [41] W. Humphrey, A. Dalke, and K. Schulten, *J. Mol. Graphics* **14**, 33 (1996).
- [42] C. Pastorino, T. Kreer, M. Müller, and K. Binder, *Phys. Rev. E* **76**, 026706 (2007).
- [43] H. J. Limbach, A. Arnold, B. A. Mann, and C. Holm, *Comput. Phys. Commun.* **174**, 704 (2006).
- [44] A. Arnold, O. Lenz, S. Kesselheim, R. Weeber, F. Fahrenberger, D. Roehm, P. Košovan, and C. Holm, in *Meshfree Methods for Partial Differential Equations VI*, edited by M. Griebel and M. A. Schweitzer, Lecture Notes in Computation Science and Engineering, Vol. 89 (Springer, Berlin, 2013), pp. 1–23.
- [45] T. Bickel and R. Bruinsma, *Biophys. J.* **83**, 3079 (2002).
- [46] R. Y. H. Lim, B. Fahrenkrog, J. Koeser, K. Schwarz-Herion, J. Deng, and U. Aebi, *Science* **318**, 640 (2007).